Per. Mineral. (2010), 79, 1, 1-25

doi: 10.2451/2010PM0001
http://go.to/permin

PERIODICO di MINERALOGIA
established in 1930

An International Journal of
MINERALOGY, CRYSTALLOGRAPHY, GEOCHEMISTRY, ORE DEPOSITS, PETROLOGY, VOLCANOLOGY
and applied topics on *Environment*, *Archeometry* and *Cultural Heritage*

Ejected rocks from the 1872 eruption of Vesuvius, Italy: a petrographic and mineralogical overview

Carmela Petti[1], Giuseppina Balassone[2,*], Alessandro Maria Bernardi[2], Angela Mormone[2], Manuela Rossi[2] and Maria Rosaria Ghiara[1,2]

[1]Reale Museo Mineralogico, Centro Musei delle Scienze Naturali Università degli Studi di Napoli Federico II, Via Mezzocannone 8, 80134 Napoli, Italy
[2]Dipartimento di Scienze della Terra, Università degli Studi di Napoli Federico II, Via Mezzocannone 8, 80134 Napoli, Italy

Submitted, July 2009 - Accepted, February 2010

Abstract - A set of 30 ejecta from the 1872 eruption of Vesuvius have been selected in the Scacchi's collection of the Real Mineralogical Museum of University Federico II (Naples) to study their petrographic and mineralogical features and to provide insight into their genetic processes. Petrographic study has established the occurrence of four varieties: 1) homogenous lavas (HL); 2) composite lavas (CL); 3) lavas and/or metamorphic rocks macroscopically conglomerate-like (LMC); 4) conglomerates (C). Mineral chemistry investigation has shown that the samples investigated consist of a large number of phases. These include minerals which typically occur in the Somma-Vesuvius lavas, like clinopyroxene, leucite (and other feldspathoids), plagioclase, K-feldspar and trioctahedral mica. Moreover a number of late to post-magmatic phases also occur. Textural, petrographic and mineral chemistry evidences indicate that phase crystallization are the result of a number of processes and complex interactions between rising lava, lava protholits and pulse of hydrothermal fluids and fumaroles at variable temperature and composition.

Riassunto - I caratteri mineralogici e petrografici di trenta proietti vesuviani provenienti dall'episodio eruttivo del 1872 e conservati presso la Collezione Scacchi del Reale Museo Mineralogico di Napoli (Università Federico II) sono stati studiati al fine di stabilire i loro aspetti genetici. Lo studio petrografico ha evidenziato la presenza di quattro diversi litotipi, quali lave omogenee (HL), lave composite (CL), lave e/o rocce metamorfosate, macroscopicamente assimilabili a conglomerati (LMC) e conglomerati (C). Lo studio composizionale ha mostrato una varietà di fasi mineralogiche che includono in prevalenza minerali di origine ignea tipici del Somma-Vesuvio, come clinopirosseno, leucite (ed altri feldspatoidi), plagioclasio, feldspato potassico e mica triottaedrica. Sono altresì presenti diverse fasi da tardo a post-magmatiche. Le evidenze tessiturali, petrografiche e composizionali indicano che i processi minerogenetici sono il risultato di vari processi e complesse interazioni tra lava in risalita e protoliti lavici con fluidi idrotermali ed emissioni fumaroliche caratterizzati da variabile temperatura e composizione.

Key Words: *Somma-Vesuvius, A.D. 1872 eruption, ejecta, Mineralogical Museum of Naples, petrographic features, mineral chemistry.*

Introduction

Somma-Vesuvius, the most famous among the

* Corresponding author, E-mail: balasson@unina.it

volcanoes located in the Campania region, is extensively investigated for its magmatological and volcanological history (Di Renzo *et al*., 2007). Variable composition of the magmatic series (slightly silica-undersaturated to highly silica-undersaturated and from potassic to ultrapotassic affinity), variable eruptive styles and cyclicity are characteristic of this polygenic stratovolcano. Effusive lava flow and scoria eruptions, the most common type of volcanism during the last 3.5 ka, alternated to highly explosive plinian eruptions of pumice and ash, associated with pyroclastic flows and surges.

Notably a wide variety of xenoliths often related to pyroclastics of plinian eruptions are found as ejected rocks. Several mineralogical and petrological studies have been carried out by many research groups, and six common varieties of ejecta can be identified: "accumulative" rocks (biotite-bearing pyroxenite, wehrlite and dunite), metasomatized carbonatites, skarns, hornfels, shallow plutonic rocks, lavas, sedimentary rocks. Comprehensive reviews of Somma-Vesuvius nodules have been recently given by Cigolini (2007 and reference therein) and Lima *et al.* (2007 and reference therein). It is well established that xenoliths from volcanic rocks represent a valuable source of information on the composition of deep-seated rocks and on volcanic processes (Federico and Peccerillo, 2002).

Different eruptive cycles have been recognized at Somma-Vesuvius. The so-called *Recent* activity refers to the last eruptive events occurring between A.D. 1631 and 1944, which comprise all the exposed lavas (Rolandi *et al*., 1993; Lirer *et al*., 2005; Santacroce *et al*., 2005). Starting from 1944, the volcano has been quiescent, with only moderate seismicity and fumarolic phenomena. Between 1631 and 1872, 99 magmatic eruptions were reported and the explosive activity was predominant (Scandone *et al.*, 2006). During 1872 the Somma-Vesuvius produced one of the most violent eruptions of the XIX century, which was preceded by many eruptive events (1868, 1861 and 1858. Lirer *et al.,* 2005). This eruption has been classified as "explosive/effusive". Immediately after the effusive stage eyewitness observations described a strong explosive activity with the ejection of many rocks (Palmieri, 1872;1873; 1874).

New findings of rare mineral species in some of the1872 ejecta (Balassone *et al*., 2004; Ghiara, 2005; Petti, *et al*., 2008; Balassone *et al*., 2008), prompted the necessity of further research. The rediscovery of 480 samples in the Real Mineralogical Museum of the University of Naples (RMMN), which were collected by the director Arcangelo Scacchi mainly during 1873, provided a unique opportunity to investigate the nature of these poorly studied rocks. In fact the RMMN specimens were only partly described by Scacchi and his son (Scacchi, 1872a, b; 1873; Scacchi and Scacchi, 1883). In this paper we present new petrographic, geochemical and mineralogical data on representative samples of the Scacchi's collection, sheding light on their genesis and processes occurring at the magma-hydrothermal system interface.

The A.D. 1872 eruption and the Scacchi's samples

The recent eruptive history of Somma-Vesuvius is characterized by semi-persistent, relatively mild activity frequently interrupted by quiescent periods, occurring in short cycles represented by the four-stage sequence calm→intermediate eruption→strombolian activity→final eruption (Arnò *et al.,* 1988). The 1870-1872 period was classified as a lateral eruption. On April 26 a new deep NW-trending fracture opened in the flank of the volcano, extending for 300 meters at the "Atrio del Cavallo". In the first stage, leucite-rich ashes emission occurred, followed by fluid lava effusions. Lava flows directed towards the towns of Ercolano, San Sebastiano and Cercola, mostly covering older lava deposits. Then, a second fracture opened in the southern sector of the Vesuvian cone and a new lava flow moved

towards Camaldoli (Torre del Greco, Fig. 1). Strong explosions occurred overnight, with lithics thrown up to about six kilometres (Palmieri, 1880). On April 27 explosive activity continued unevenly whereas lava effusions stopped. Explosive eruptions occurred until May 1st and afterwards a white cloud was observed and numerous fumarolic emissions took place mainly between the royal palace of Portici and the locality called "La Favorita". Joron *et al.* (1988) reported for the 1872 lavas a prevailing leucititic tephrit-phonolite composition, with mineralogical paragenesis represented by large phenocrysts of leucite, clinopyroxene and minor plagioclase set in a groundmass (holo- to hypocrystalline to glassy) showing variable amounts of leucite, clinopyroxene, Ca-plagioclase, mica, apatite and opaques.

Arcangelo Scacchi, worldwide famous mineralogist of the nineteenth century, demonstrated a great scientific interest for the 1872 rocks of the RMMN, which he used to take to his lectures. It is worth to note that the mineralogical importance of the 1872 specimens also lies in the first finding of mineral species microsommite and erythrosiderite made by Scacchi himself (Scacchi, 1872a; Russo and Punzo, 2004). He gave a first description of all specimens by visual observation, reporting in their labels sometimes the main lithologic feature, or the mineral assemblage or only one prevailing mineral. Scacchi classified most of the RMMN

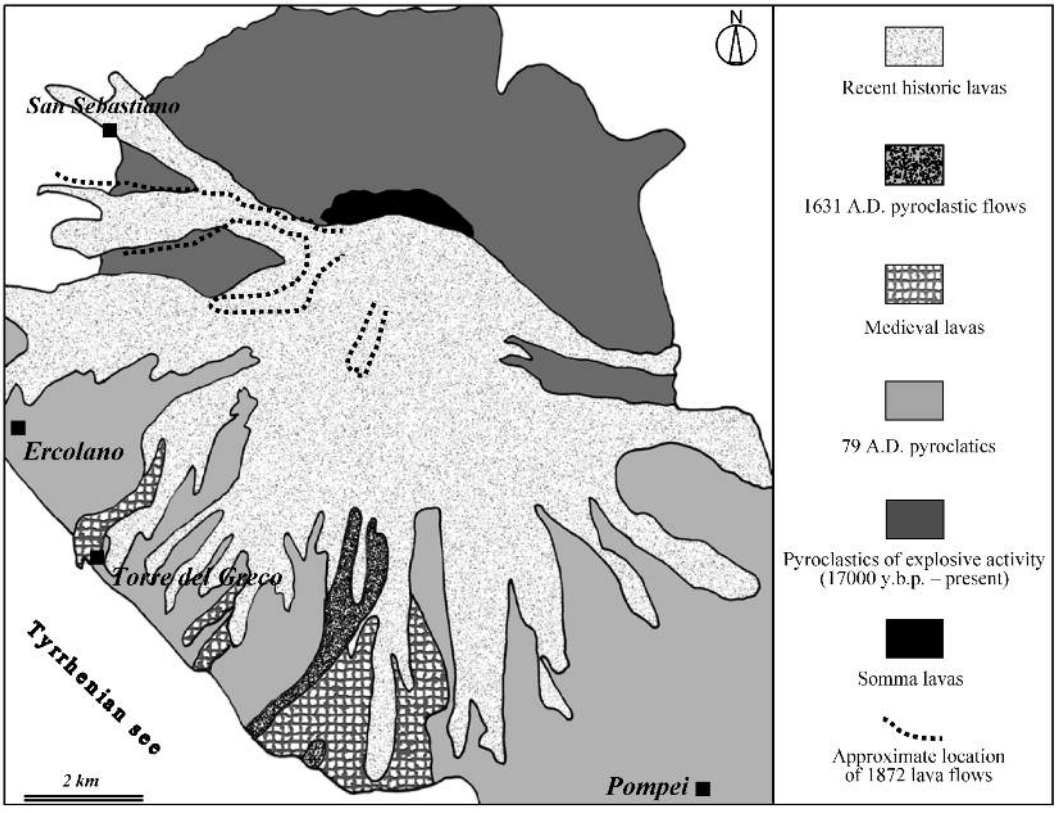

Fig. 1 - Schematic geo-volcanological map of Somma-Vesuvius (redrawn after Ayuso *et al.,* 1998).

rocks as ejecta and established the predominance of two lithologies, i.e. lavas and conglomerates (Scacchi, 1886; 1888). He also described some striking mineralogical and petrographic features that were related to contact metamorphism and post-magmatic processes, the latter mostly due to hydrothermal and fumarolic activity. Finally, Scacchi proposed that rock types could represent uncommon and very promising samples in the petrological and volcanological frame of Somma-Vesuvius, since some mineralogical and petrographic features were observed for the first time among vesuvian products.

Analytical methods

For the present study a total of 30 representative samples selected by hand specimen examination have been selected from the Scacchi's collection (Table 1). Optical microscopy (OM) was used for petrographic description in thin section. The identification of various phases of the mineral assemblages has been determined by OM, X-ray diffraction (XRD), scanning electron microscopy (SEM) and microanalysis with energy dispersive (EDS) and wave dispersive (WDS) spectrometry. XRD on powders and single crystals (Gandolfi method) were performed with a Seifert-GE MZVI diffractometer under the following conditions: CuKα radiation at 40 kV and 30 mA, 2 and 1 mm divergence slits, 1 mm receiving slit 0.1 mm, antiscatter slit 1 mm, step scan 0.05°, counting time 5 sec/step. The software package RayfleX (GE Inspection Technologies, 2004) was used for data processing and phase identification was carried out using the ICDD-PDF2 database. Morphological examination and qualitative-quantitative chemical analyses have been performed by a SEM JEOL-JSM 5310 instrument equipped with a Link EDS and using natural and synthetic standards (CISAG - University Federico II, Naples). Operating conditions were 15kV accelerating voltage and 10μm spot size Data were processed with the software Link AN10000 and INCA version 4.08 (Oxford Instrument, 2006). Selected samples were analysed by a full WDS microprobe Cameca SX50 electron microprobe (IGAG CNR, Rome), operating at an accelerating voltage of 15kV, 15nA beam current and 10 to 20 μm spot size. Data were corrected using the PAP program (Pouchou and Pichoir, 1991). Minerals and pure elements were used as standards.

Results

Petrography

The petrographic description of the 30 samples of the Scacchi's 1872 collection is based on both macroscopic textures and OM study in thin section. In some cases differences between specimens are not so sharp and attribution to one or another type can be quite problematic. This can be due to texture obliteration for a deep hydrothermal alteration and/or sub-millimetric transitions among various lithologies. For discussion's sake the specimens have been grouped in four varieties (Table 1): homogenous lavas (HL), composite lavas (CL), lavas and/or metamorphic rocks macroscopically conglomerate-like (LMC) and conglomerates (C).

HL type. Homogenous lava samples show compact to vesiculated textures, up to scoriaceous. Eleven samples belong to this rock type, which is the most represented of the Scacchi's collection, together with the LMC type. A typical lithology is shown in Fig. 2a. They have a wide compositional spectrum ranging from basic to felsic rock-types, like basanites, tephriphonolite and phonolites. Lavas normally exhibit a porphiritic texture, often seriate, and holocrystalline to glassy groundmass. Tephritic lavas (i.e. sample # D1381 10930) show leucite and/or diopsidic clinopyroxene phenocrysts in a groundmass of clinopyroxene and leucite with minor sanidine and plagioclase (Fig. 3a). Opaque

TABLE 1

Catalog numbers of RMMN 1872 samples investigated for this study, their lithotypes, and main mineral phase.

#	*catalog nr.*	*lithotype**	*main minerals***
1	D1381 10930	HL	cpx, lct, fld, ol, mgt, hem, ap
2	D1400 10949	HL	cpx, fld, mgt, hem, sdl
3	D1423 10972	HL	lct, fld, cpx, mi, gp, anh, hl
4	D1434 10983	HL	cpx, lct, mi, amp, ol, fld, gp, anh
5	D1467 11016	HL	lct, cpx, fld, mi, gp
6	D1468 11017	HL	lct, cpx, mgt, anh
7	4D	HL	cpx, lct, fld, mgt, hem, gp, anh
8	5D	HL	cpx, lct, fld, mgt, hem
9	6D	HL	cpx, lct, fld, mgt, hem
10	7D	HL	cpx, lct, fld, mi, mgt, hem, gp, anh
11	9D	HL	lct, fld, cpx, hl, anh
12	D1403 10953	CL	cpx, fld, amp, sld, ap, mgt, hem, sy
13	D1418 10967	CL	cpx, lct, fld, ap, mgt, hem, hl
14	D1464 11013	CL	cpx, fld, lct, mgt, hem, gp
15	D1422 10971	LMC	cpx, mi, lct, fld, mgt, hem
16	D1433 10982	LMC	cpx, lct, mi, fld, mgt, hem, ap
17	D1453 11002	LMC	cpx, fld, lct, mgt, hem
18	D1458 11007	LMC	cpx, lct, mi, mgt, hem
19	D1460 11009	LMC	lct, fld, cpx, mgt, hem
20	D1470 11019	LMC	cpx, lct, hl
21	D1502 11051	LMC	cpx, lct, amp, sdl, ccn
22	E5652 17113	LMC	cpx, amp, lct, sdl, ap, mgt, hem
23	E5876 17337	LMC	lct, fld, cpx, mi, ccn, ap, mgt, hem
24	E5877 17338	LMC	lct, cpx, fld, mi, ccn, ap, mgt
25	2D	LMC	cpx, lct, hem
26	3D	LMC	mi, mgt, hem, fld, osm, ind, cpx, sdl, ap, crs
27	D1419 10968	C	lct, cpx, mi, hem, mgt, gp, hl
28	D1429 10978	C	cpx, lct, fld, mgt, hem, mi, amp
29	D1436 10895	C	cpx, lct, amp, sdl, ap, mgt, hl
30	D1463 11012	C	fld, cpx, lct, mi, ol, mgt, hem, gp

* see text for acronym explanation.

** detected by combined optical microscopy and X-ray diffraction, and listed in order of decreasing abundance.

Cpx, clinopyroxene; lct, leucite; fld, feldspars; mi, mica; ol, olivine; amp, amphibole; mgt, magnetite; hem, hematite; ilm, ilmenite; ap, apatite; sdl, sodalite-group minerals; ccn, cancrinite-group minerals; hl, halite; sy, sylvite; gp, gypsum; anh, anhydrite; osm, osumilite; ind, indialite; crs, cristobalite. Symbols partly after Kretz, 1983.

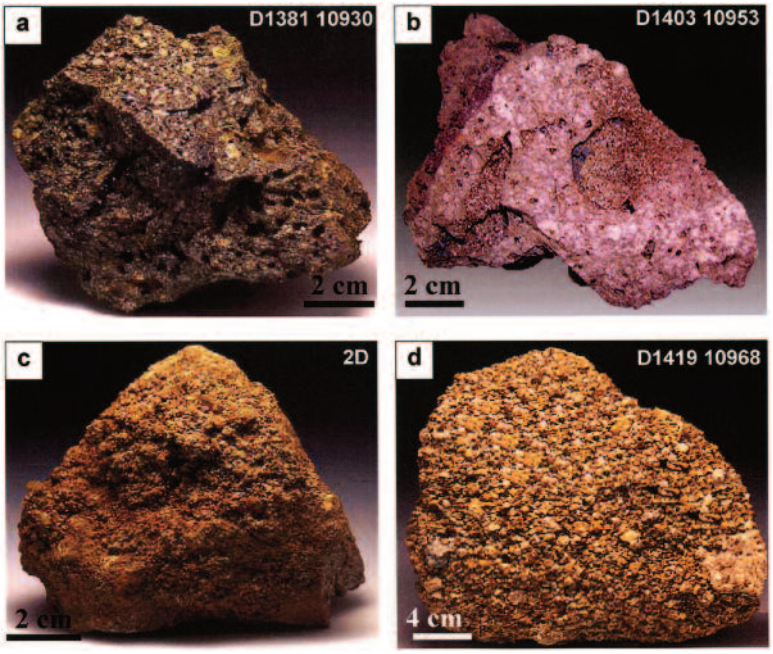

Fig. 2 - Selected lithologies from1872 eruption: (a) HL, (b) CL, (c) LMC, (d) C (see Table 1 for label explanation).

minerals (mainly hematite and magnetite) and apatite can occur as accessory phases. Relics of forsteritic olivine and *ocelli* of potassic feldspar are also observed locally. Clinopyroxenes can be mantled by pargasitic amphibole, also occurring in cavities in association with tiny light brown mica laths and rare gypsum and/or anhydrite. Few phonothephrite samples present a highly vesiculated texture with a phenocrysts association represented by leucite (sometimes with dark inclusions), clinopyroxene, amphibole, sanidine. In some specimens late to post-magmatic alteration locally led to the growth of sodalite, hematite, magnetite, anhydrite, gypsum and halite in the vesicles.

CL type. This rock type exhibits more or less sharp transitions in handspecimen between lavas with different petrographic and textural features (Fig. 2b). In Fig. 3b a porphiritic seriate holocrystalline lava (sample # D1403 10953) abruptly changes to a vitrophiric vesiculated lava. Phenocrysts of leucite, locally with glass inclusions, are widespread in both lavas, followed by clinopyroxene; microphenocrysts of leucite, clinopyroxene and plagioclase form the groundmass of the holocrystalline lava and also occur in the vitrophiric lava. Hematite mainly occurs as vein and cavity lining. Structural evidences at the contact zone clearly indicates the typical features of a rapid cooling, likely due to incorporation of solid and/or semisolid material by a melt.

LMC type. LMC are rather heterogeneous rocks and they can be manly represented by lava+scoria+conglomerates (Fig. 2c). Some samples are characterized by a lava core completely enveloped by a clastic fraction, as widely described by Scacchi (1886). Fig. 3c displays a representative LMC sample (# D1433 10982), with a scoria fragment resting on a lava. Lava is a phonolitic tephrite and is glomeroporphyritic holocrystalline; phenocrysts

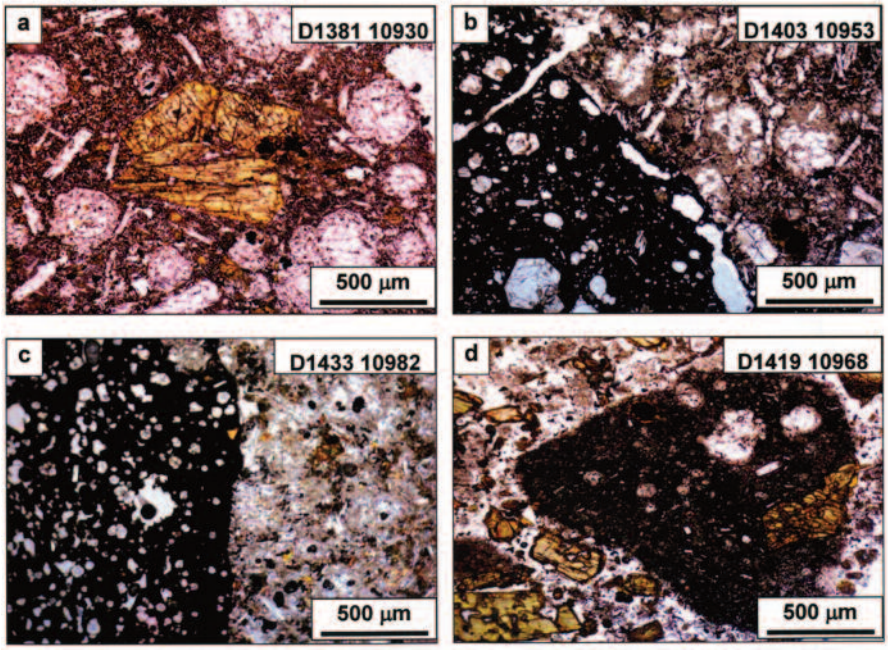

Fig. 3 - Micrographs in thin section of representative rock types (see text for petrographic descriptions).

are plagioclase, clinopyroxene (salite), amphibole and mica. The *ocelli* have a K-feldspar core and a plagioclase rim. Conglomeratic fraction is composed by small lava lithics and loose crystals of leucite and clinopyroxene with interstitial hematite. The scoria shows phenocrysts of clinopyroxene and leucite rich in glassy inclusions. In the glassy matrix, microphenocrysts of mica, plagioclase, amphibole, apatite and opaques can be observed. The occurrence of a glassy chilled margin in the welding area between scoria and lava suggests that the latter incorporated the hot scoria. Other LMC samples show the conglomeratic fraction resting on a tephritic lava. Lavas show porphyric seriate textures, phenocrysts of leucite and clinopyroxene and microphenocrysts of leucite (locally altered), clinopyroxene and plagioclase are observed. Tiny hedenbergite and kaersutite also occur in the groundmass. Leucite is often characterized by many reddish-black inclusions, particularly rich in iron (~11 wt% FeO) and titanium (~1.2 wt% TiO_2). Conglomeratic fraction is crumbly and generally formed by small lithics (lava fragments) and loose crystals (mostly clinopyroxene and hematite). Fine-grained matrix is always very scarce and composed by variable amounts of leucite, clinopyroxene, mica, sodalite- cancrinite group minerals, amphibole, hematite, magnetite, Ca-sulfates (gypsum and anhydrite) and halides (halite and sylvite). Some LMC rocks are particularly rich in feldspathoids of the sodalite and cancrinite groups, which also occurs in vugs and encrustations.

One LMC sample (# D3) can be described as pumice/lava clasts aggregates. Pumice clasts (up to ~3-4 cm) display a mineral assemblage given by tiny phlogopite, sanidine, clinopyroxene, sodalite, Ca-sulfates and apatite, whereas indialite, osumilite and cristobalite are mainly concentrated in whitish thin crusts covering the

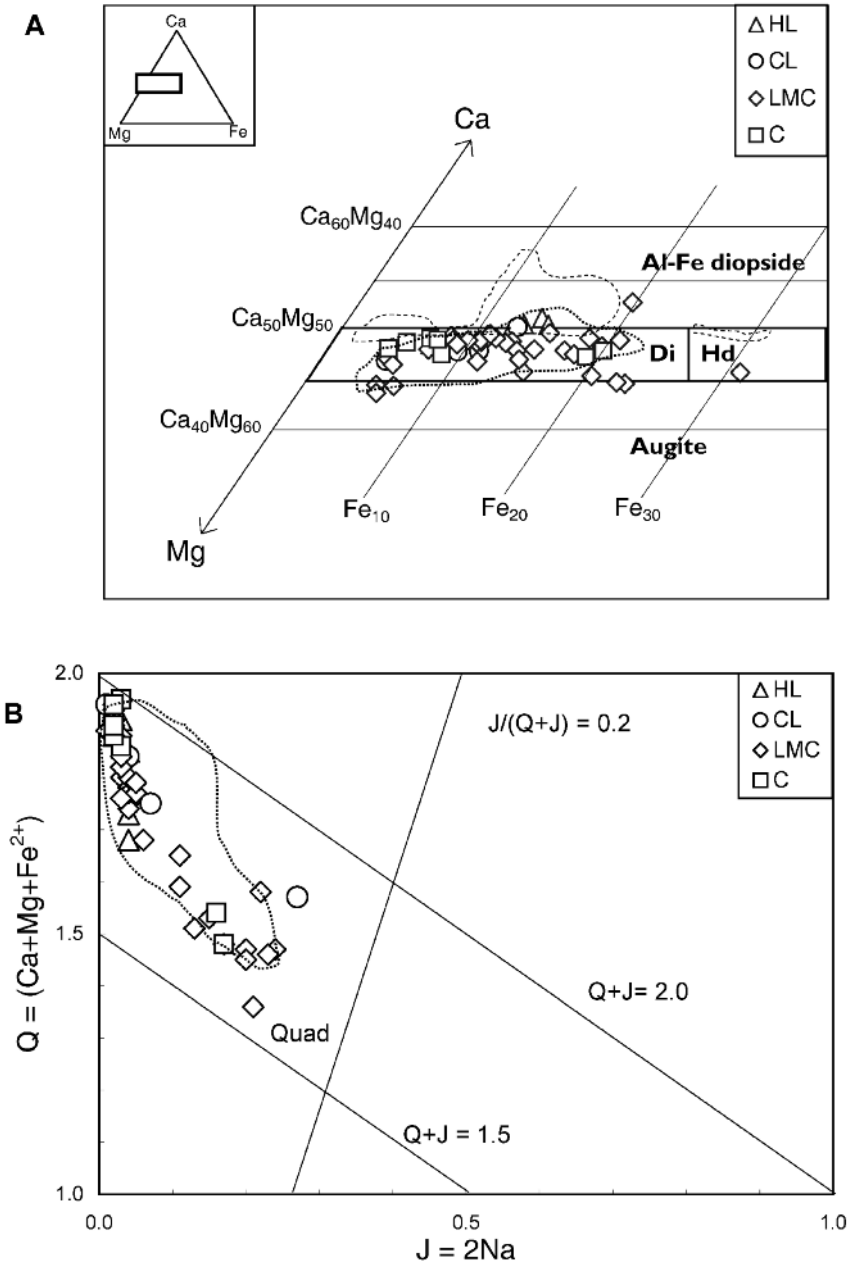

Fig. 4 - A) Clinopyroxenes from selected samples plotted within the Ca-Mg-(Fe^{2+} + Fe^{3+} + Mn) diagram. B) Q-J diagram for clinopyroxenes from the 1872 samples, according to Morimoto *et al.* (1988). The dotted fields show the composition of clinopyroxenes of 1631-1944 vesuvian lavas (from Solone, 2006), whereas the dashed fields represent the composition of the Somma-Vesuvius skarn clinopyroxenes after Gilg *et al.* (2001).

clasts. Black spots are formed by hematite and magnetite. This rock is quite similar to samples already described by Balassone *et al.* (2004, 2008).

C type. The C lithology corresponds to monogenic and polygenic friable conglomerates (Fig. 2d). It is characterized by lithic fraction (maximum dimension of ~1.5 cm) and loose crystals, i.e. ubiquitous leucite and clinopyroxene. Conglomerate matrix is always scarce and fine grained and composed by variable percentages of the same minerals already observed in the LMC lithology. A typical C sample (#D1419 10968) is presented in Fig. 3d. Lithics are polygenic and represented by three lithologies: vitrophiric fragments, lava lithics with phenocrysts of clinopyroxene, leucite, plagioclase, mica and ilmenite in a glassy matrix, lithics with mica, plagioclase, K-feldspar and magnetite in a microcrystalline groundmass. Clinopyroxene is always strongly zoned, with a hedenbergitic (Fe-salite) rim and a diopsidic core, and often mantled by hornblende amphibole and locally showing inclusions of apatite.

Mineral chemistry

Clinopyroxene occurs in all the investigated rocks as euhedral to anhedral crystals, in some cases as relics (Table 1). Representative microanalyses are reported in Table 2 and the pyroxene formulas and nomenclature follow Morimoto *et al.* (1988). Their compositions have been plotted in Ca-Mg-(Fe^{2+},Fe^{3+},Mn) diagram (Fig. 4a). Clinopyroxenes from HL and CL types show a quite similar composition and mainly plot in the diopside field (salite-diopside), with only few samples crossing over the Wo_{50} divide (in the field of subsilicic ferroan aluminian diopsides, "fassaites"). They overlap with the area of clinopyroxenes from lavas related to *recent* activity of Vesuvius (A.D. 1631-1944; Solone, 2006; Marianelli *et al.,* 1999; Cioni *et al.,* 1998; Fulignati *et al.,* 1998; Santacroce, 1987). Mg-values mostly range from 0.85 and 0.98; chemical zoning is seldom observed. The analyzed samples from LMC type covers a wider compositional range, mostly varying between hedenbergite and diopside (from salite to endiopside); two samples plot on the join diopside-augite, whereas one sample shows a slight fassaitic composition. Significant chemical zoning has been also locally pointed out in clinopyroxenes of both lava and conglomerate fraction. A typical core-rim evolution trend can be $Wo_{50}Fs_{12}$ to $Wo_{46}Fs_{20}$. In another case (i.e. clinopyroxenes from lava fraction) a reverse trend has also been observed, with a $Wo_{48}Fs_{13}$ core and a $Wo_{47}Fs_{7}$ rim. Chemical zoning observed in these mineral phases is generally related to change of magmatic water pressure and/or mixing and contamination processes which influence magma composition (Aurisicchio *et al*., 1988; Conticelli *et al.,* 2002; Morgan *et al.,* 2004). Mg-values for LMC clinopyroxenes are in the range 0.79-0.94. Clinopyroxenes of C type mainly cluster at about $Wo_{48}Fs_{7}$ and $Wo_{47}Fs_{20}$. Chemical zoning is locally observed. Mg-values of these minerals vary between 0.91 and 0.92. On the basis of the Morimoto's et al. (1988) classification, all the studied clinopyroxenes plot in the Quad area in the Q-J diagram (Fig. 4b).

Mica occurs in several samples of the various rock types, both in the groundmass and as microphenocrysts, locally occurring with corroded rims. Representative microprobe analyses are reported in Table 3a. In the "ideal biotite plane" defined by phlogopite-annite-eastonite-siderophyllite end-members (Guidotti, 1984) and in agreement with the classification of Rieder *et al.* (1998) the investigated micas (HL, CL, LMC and C types) fall in the field of the phlogopitic composition (Fig. 5a); almost all samples are in the ranges ^{IV}Al 0.002-0.200 apfu and Mg-value 0.73-0.83. Only LMC mica of sample # D3 is distinctly Mg-rich, with a Mg-value of about 0.98. In the TiO_2 *vs* Al_2O_3 diagram, most of micas plot in a field characterized by 4.0-

Table 2
Selected electron microprobe analyses and structural formulae (apfu) of clinopyroxenes in the HL, CL, LMC and C rock types.

Type	HL				CL		LMC								C		
Sample #	D1400 10949		D1423 10972	7D	D1418 10967	D1464 11013	D1433 10982		D1458 11007		D5652 17113		E5877 17338		D1419 10968	D1436 10895	
	core	rim					core	rim	core	rim	core	rim	core	rim		core	rim
SiO_2	52.04	47.18	54.82	44.24	47.31	49.25	53.46	46.89	49.2	49.07	54.00	47.66	52.03	47.85	51.82	51.19	51.74
TiO_2	0.59	1.21	0.35	1.84	1.06	0.95	0.61	1.42	0.97	0.77	0.17	1.04	0.52	0.73	0.39	0.64	0.58
Al_2O_3	2.56	6.03	1.51	8.54	6.27	6.21	2.07	7.63	5.07	5.22	1.64	6.95	3.09	4.94	2.86	2.95	2.52
FeO*	4.46	7.65	3.53	8.67	7.44	6.26	4.12	8.04	6.46	6.65	3.23	7.01	4.66	10.07	5.29	4.81	4.4
MnO	0.16	0.18	0.1	0.16	0.15	0.15	0.14	0.10	0.17	0.15	0.09	0.18	0.11	0.62	0.30	0.12	0.12
MgO	15.58	12.30	17.55	11.58	12.34	13.16	17.19	12.63	14.32	14.16	17.62	13.44	15.93	11.41	15.89	15.54	15.66
CaO	23.66	23.55	20.97	23.22	23.07	21.19	21.57	21.78	23.60	23.60	23.91	23.29	23.70	21.73	23.81	24.22	24.19
Na_2O	0.18	0.30	0.12	0.25	0.45	1.87	0.14	0.24	0.22	0.21	0.11	0.28	0.19	1.52	0.19	0.15	0.12
Total	99.23	98.40	98.95	98.50	98.09	99.04	99.30	98.73	100.01	99.83	100.77	99.85	100.23	98.87	100.55	99.62	99.33
Fe_2O_3**	0.96	4.24	-	6.48	4.12	6.61	-	2.58	4.12	4.32	1.28	4.85	1.92	8.59	3.32	2.86	1.77
FeO**	3.60	3.83	3.53	2.84	3.73	0.95	4.12	5.71	2.75	2.77	2.08	2.65	2.93	2.02	2.30	2.24	2.81
Cations per 6 O																	
Si	1.922	1.782	1.998	1.674	1.788	1.814	1.957	1.763	1.813	1.813	1.947	1.762	1.900	1.799	1.889	1.884	1.909
AlIV	0.078	0.218	0.002	0.326	0.212	0.186	0.043	0.237	0.187	0.187	0.053	0.238	0.100	0.201	0.111	0.116	0.091
AlVI	0.033	0.051	0.063	0.055	0.067	0.084	0.046	0.101	2.770	0.040	0.017	0.650	0.033	0.018	0.012	0.012	0.018
Ti	0.016	0.034	0.01	0.052	0.030	0.026	0.017	0.040	0.021	0.021	0.005	0.029	0.014	0.021	0.011	0.018	0.016
Fe3+	0.027	0.121	-	0.184	0.117	0.183	-	0.073	0.120	0.120	0.035	0.135	0.053	0.253	0.091	0.079	0.04
Fe^{2+}	0.111	0.121	0.108	0.090	0.118	0.01	0.126	0.180	0.085	0.085	0.063	0.082	0.089	0.063	0.070	0.069	0.018
Mn	0.005	0.006	0.003	0.005	0.005	0.005	0.004	0.003	0.005	0.005	0.003	0.006	0.003	0.020	0.005	0.004	0.004
Mg	0.858	0.693	0.954	0.653	0.695	0.723	0.938	0.708	0.780	0.780	0.947	0.741	0.867	0.639	0.864	0.853	0.861
Ca	0.936	0.953	0.819	0.941	0.934	0.836	0.846	0.877	0.934	0.934	0.924	0.923	0.927	0.875	0.930	0.955	0.956
Na	0.014	0.022	0.008	0.018	0.033	0.134	0.010	0.017	0.015	0.015	0.008	0.020	0.013	0.111	0.013	0.011	0.009
mg	0.884	0.851	0.899	0.879	0.855	0.987	0.881	0.798	0.903	0.901	0.938	0.900	0.906	0.910	0.925	0.925	0.909
Mg	44.3	36.6	50.6	34.9	37.2	41.2	49.0	38.4	40.9	40.6	48.0	39.3	44.7	34.5	44.0	43.5	44.0
ΣFe	7.4	13.1	5.9	14.9	12.8	11.2	6.8	13.9	10.6	10.9	5.1	11.8	7.5	18.2	8.7	7.8	7.1
Ca	48.3	50.3	43.5	50.2	50.0	47.6	44.2	47.7	48.5	48.5	46.9	48.9	47.8	47.3	47.3	48.7	48.9
Na	12.6	8.0	42.4	4.6	12.0	38.6	14.2	5.9	6.9	6.7	11.8	7.0	10.5	33.3	9.9	7.4	7.4
Al^{IV}	72.3	79.5	9.7	82.2	77.0	53.8	61.8	80.5	81.4	83.7	81.1	82.9	78.4	60.5	82.2	80.3	78.7
Ti	15.1	12.5	47.9	13.2	11.0	7.6	24.0	13.6	11.7	9.6	7.1	10.1	11.1	6.2	7.9	12.3	13.9

* Total FeO as FeO; ** calculated according to Papike *et al.* (1974); mg = $Mg/(Mg+Fe^{2+})$; $\Sigma Fe=Fe^{2+}+Fe^{3+}+Mn$

5.5 wt% TiO_2 and 16.0-16.5 wt% Al_2O_3. Mg-rich LMC mica and a HL sample, also found in cavities of a tephritic lava, are Ti and Al-poor ranging between ~2.0-0.7 wt% TiO_2 and 10.1-10.0 wt% Al_2O_3. Barium was detected in almost all the studied trioctahedral micas, in a range 0.1-1.7 wt% BaO. They finally display wide variation in fluorine content (0.36-3.38 apfu F), with the F-(and Mg) rich micas coming from the LMC pumice aggregates.

Amphiboles have been randomly detected in the various lithologies, and selected chemical analyses are showed in TABLE 3b. In some samples, they mantle clinopyroxene phenocrystals. According to classification of Leake *et al.* (1997, 2004), their compositions mostly fall in the fields of the calcic amphiboles Mg-hornblende, tschermakite and pargasite (Fig. 5b). One LMC sample, classified as Fe-tschermakite for its contents of $Ca_B \geq 1.5$ apfu (2.00 apfu), Na_B<0.50 apfu (no Na assigned to B-site), $(Na+K)_A$ < 0.50 apfu (0.27 apfu) and Ti<0.50 apfu (0.23 apfu), shows an amount of $Fe^{3+} > Al_C$ (Fe^{3+} 0.24 apfu against Al_C 0.0 apfu)

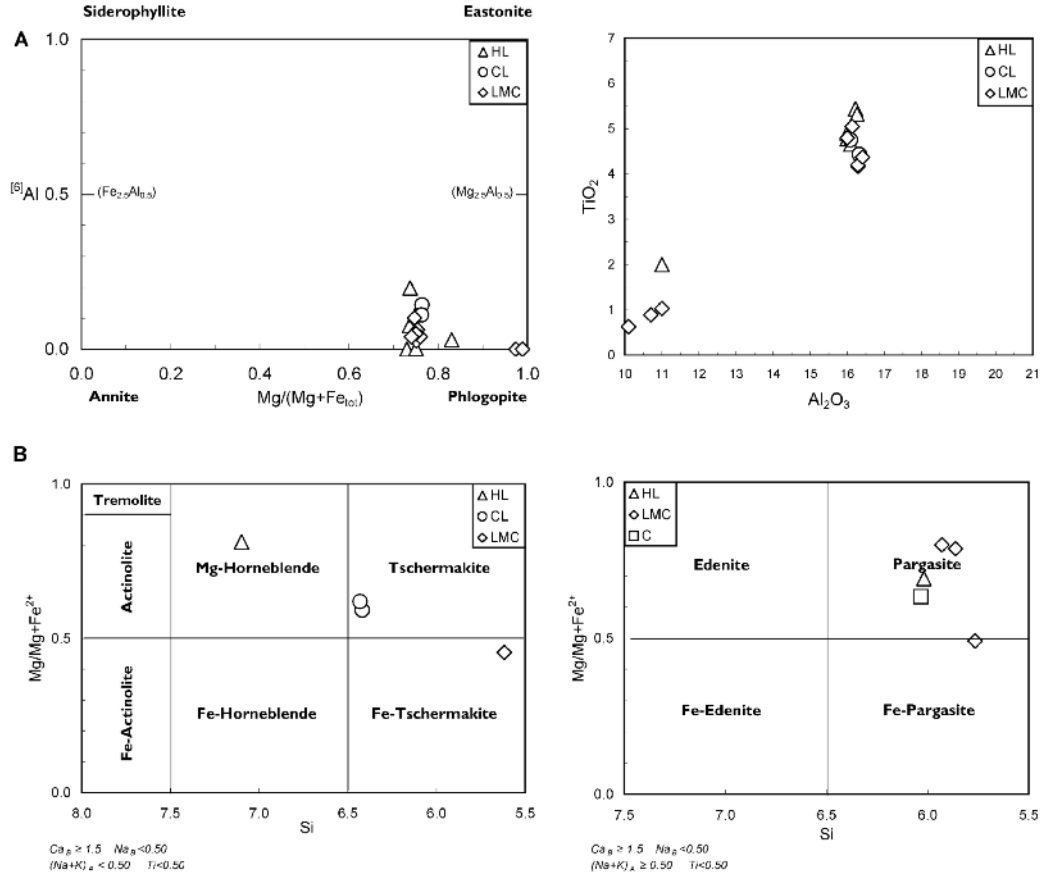

Fig. 5 - A) Compositional variation for trioctahedral micas of this study plotted in the phlogopite-annite-siderophyllite-eastonite plane (atoms per formula units, apfu) diagram (Rieder *et al.,* 1998), and in TiO_2 vs Al_2O_3 diagram (in wt%). B) Compositional variations of Ca- and Ca-Na amphiboles of the studied samples, according to the classification of Leake *et al*. (1997, 2004).

Table 3
WDS analyses and structural formulae (apfu) of selected micas (a) and amphiboles (b) in the different lithologies from the 1872 eruption.

(a)

Type	HL	HL	HL	HL	CL	LMC	LMC	LMC	LMC
Sample #	D1434 10983	D1467 11016	D1468 11017	7D	D1403 10953	D1433 10982	E5876 17337	D3	D3
SiO_2	41.30	36.72	35.91	34.38	36.27	36.27	36.15	43.58	43.07
TiO_2	2.00	4.91	4.78	5.44	4.75	4.17	4.80	1.03	0.63
Al_2O_3	11.00	16.00	16.00	16.22	16.09	16.29	16.00	11.00	10.10
FeO*	7.46	10.45	10.31	10.45	9.76	10.57	10.50	1.30	0.68
MnO	0.17	-	0.07	0.13	0.04	0.06	0.02	0.04	0.03
MgO	20.33	16.45	17.22	16.34	17.77	17.85	17.36	27.13	26.65
CaO	0.07	0.10	0.11	0.11	0.05	-	0.04	0.03	0.02
BaO	0.68	1.59	1.35	1.74	1.48	1.43	1.60	0.09	-
Na_2O	0.51	0.29	0.30	0.33	0.31	0.30	0.24	0.28	0.22
K_2O	9.49	9.01	9.35	9.02	8.58	9.28	9.49	9.64	9.20
F	6.36	0.76	1.30	0.86	1.00	1.02	0.91	7.59	7.08
Cl	-	0.08	0.05	0.07	0.05	0.02	0.07	0.15	0.09
Total	*99.37*	*96.36*	*96.75*	*95.09*	*96.15*	*97.26*	*97.18*	*101.86*	*97.77*
				Ions per 22 O					
Si	6.113	5.417	5.318	5.191	5.347	5.324	5.322	6.138	6.260
Al^{IV}	1.887	2.583	2.682	2.809	2.653	2.676	2.678	1.862	1.730
Al^{VI}	0.032	0.198	0.111	0.077	0.143	0.142	0.098	-	-
Ti	0.223	0.545	0.532	0.618	0.527	0.460	0.531	0.109	0.069
Fe_t	0.924	1.290	1.277	1.320	1.204	1.298	1.293	0.153	0.083
Mn	0.021	-	0.009	0.017	0.005	0.007	0.002	0.005	0.004
Mg	4.486	3.618	3.802	3.678	3.906	3.906	3.810	5.696	5.774
Ca	0.011	0.016	0.017	0.018	0.008	-	0.006	0.005	0.003
Ba	0.039	0.092	0.078	0.103	0.085	0.082	0.092	0.005	-
Na	0.146	0.083	0.086	0.097	0.089	0.085	0.068	0.076	0.062
K	1.792	1.695	1.766	1.737	1.614	1.737	1.782	1.732	1.706
F	2.980	0.355	0.608	0.407	0.466	0.473	0.424	3.380	3.254
Cl	-	0.020	0.013	0.018	0.012	0.005	0.017	0.036	0.022
mg	0.829	0.737	0.749	0.736	0.764	0.751	0.747	0.974	0.985
Mg/Fe	4.86	2.80	2.98	2.79	3.24	3.01	2.95	37.19	64.85
$^{IV}Al/Si$	0.31	0.48	0.50	0.54	0.50	0.5	0.50	0.30	0.28

*Total Fe as FeO; mg = $Mg/Mg+Fe_t$.

and then it might be more similar to a Mg-hastingsite-hastingsite. The A-site is usually fulfilled by K and Na, followed by Ca and sporadic Ba. Fluorine was detected in almost all samples, ranging from 0.02 to 1.56 apfu F.

As regards the possible OH content in both micas and amphiboles, it was not determined because of the small size of the grains, not suitable for specific analyses.

Leucite and feldspar-group minerals are widespread in the examined samples. Representative chemical compositions of these phases are presented in Table 4. Leucite composition is close to ideal formula, with negligible replacement of K by Na and trace amounts of Ba, Ca, Mg and Mn. Iron is frequently detected with a maximum of 1.0 wt% Fe_2O_3 in a leucite from a sample of C lithology (Table 4a). Glassy, dark brown to black inclusions (up to ~15 μm) commonly arranged in a quasi-radial or

TABLE 3
Continued...

(b)

	HL	HL	CL	CL	LMC	LMC	LMC	LMC	C
	D1434 10983	D1468 11017	D1418 10967	D1418 10967	D1502 11051	D1502 11051	E5652 17113	E5652 17113	D1436 10895
SiO_2	40.84	50.77	39.11	42.33	36.44	38.00	39.65	41.03	40.65
TiO_2	1.65	0.83	1.37	1.51	1.99	2.44	1.86	1.82	1.62
Al_2O_3	13.42	8.25	6.92	7.21	12.50	14.06	11.55	11.45	10.61
FeO**	11.37	6.45	11.57	11.71	16.75	18.19	7.88	7.58	13.33
MnO	2.35	0.15	0.28	0.30	0.56	-	0.37	0.49	0.22
MgO	14.29	15.71	9.39	10.66	7.20	9.68	16.34	16.92	12.92
CaO	11.48	15.66	21.16	22.69	22.52	11.75	11.98	11.92	12.22
BaO	-	0.03	-	0.16	-	-	0.30	0.37	0.09
Na_2O	2.66	1.23	0.90	0.92	0.90	1.94	2.58	2.79	1.75
K_2O	-	0.01	0.11	0.02	0.02	2.48	1.89	1.81	2.68
F	0.25	0.12	0.04	0.19	0.28	0.65	3.22	3.37	3.33
Cl	0.13	-	0.06	0.02	-	0.43	0.04	0.01	0.08
Total	*98.44*	*99.21*	*90.91*	*97.72*	*99.16*	*99.62*	*97.66*	*99.56*	*99.5*
				Ions per 23 O					
Si	6.018	7.099	6.418	6.439	5.618	5.765	5.862	5.930	6.034
Al^{IV}	1.982	0.901	1.338	1.292	2.271	2.235	2.012	1.950	1.856
Ti	-	-	0.169	0.173	0.231	-	-	0.120	-
ΣT	8.000	8.000	7.756	7.904	8.000	8.000	8.000	8.000	8.000
Al^{VI}	0.349	0.458	-	-	-	0.278	-	-	-
Ti	0.183	0.087	-	-	-	0.278	0.207	0.078	0.181
Fe^{3+}	-	-	-	-	0.236	0.04	-	-	-
Fe_t	1.402	0.754	1.589	1.49	1.923	2.265	0.975	0.917	1.655
Mn	0.294	0.018	0.039	0.039	0.073	-	0.047	0.061	0.028
Mg	3.140	3.275	2.297	2.417	1.655	2.189	3.602	3.646	2.859
ΣC	5.368	4.592	3.925	3.946	3.887	5.050	4.831	4.702	4.723
Ca	1.812	2.000	2.000	2.000	2.000	1.910	1.898	1.846	1.943
Na	0.188	-	-	-	-	0.090	0.102	0.154	0.057
ΣB	2.000	2.000	2.000	2.000	2.000	2.000	2.000	2.000	2.000
Ca	-	0.346	1.72	1.697	1.720	-	-	-	-
Na	0.572	0.333	0.286	0.272	0.269	0.481	0.638	0.628	0.447
Ba	-	0.002	-	0.010	-	-	0.018	0.021	0.005
K	-	0.002	0.023	0.004	0.004	0.480	0.356	0.334	0.507
ΣA	0.572	0.337	0.309	0.286	0.273	0.961	1.012	0.983	0.959
F	0.117	0.053	0.021	0.091	0.140	0.310	1.506	1.540	1.563
Cl	0.032	-	0.017	0.005	-	0.110	0.010	0.002	0.020
mg	0.691	0.813	0.591	0.619	0.454	0.491	0.787	0.799	0.633
Fe_2O_3***					1.45	0.35			
FeO***					15.43	17.87			

* Amphibole mantling a clinopyroxene core; **Total Fe as FeO; *** Calculated according to Droop (1987); *mg*=Mg/Mg+Fe^{2+}.

clock face pattern can occur in leucite phenocrysts and microphenocrysts mainly of HL, CL and LMC types. It has long been recognized that leucite can characteristically contain small inclusions (normally < 1μm). These are usually considered as glass phases which represent trapped samples of the silicate melt from which the leucite crystals formed (Mitchell, 1991).

Table 4

Representative electron microprobe analyses and structural formulae (apfu) of feldspars (a) and leucites (b) in the HL, CL, LMC and C rock types.

(a)

Type	HL	HL	HL	CL	CL	LMC	LMC	LMC	LMC	LMC	C	C
Sample #	D1468 11017 core	D1468 11017 rim	7D	D1430 10953	D1464 11013	D1433 10982	D1458 11007	D1460 11009	D1460 11009	D1502 11051	D1419 10968	D1419 10968
									dark inclusion			
SiO_2	55.37	55.29	54.95	56.22	54.70	55.95	55.79	56.04	47.64	57.81	55.91	55.95
TiO_2	-	-	0.10	-	0.06	0.15	-	0.09	1.16	-	-	-
Al_2O_3	22.55	22.51	22.49	23.05	22.02	22.95	23.29	23.22	18.26	20.58	22.81	22.15
Fe_2O_3*	0.43	0.47	0.47	0.34	0.40	0.53	0.40	0.41	11.95	0.63	0.59	1.01
MgO	0.06	0.10	-	-	0.08	-	-	-	3.80	0.40	-	-
MnO	-	0.05	-	-	-	-	-	-	0.31	-	-	-
CaO	-	-	-	-	0.27	-	-	-	1.04	0.51	-	-
BaO	0.04	0.05	0.07	0.17	-	0.21	0.04	0.03	0.31	0.05	0.14	0.03
Na_2O	0.07	0.06	0.05	0.98	0.15	0.60	0.04	0.08	1.50	1.25	0.87	0.05
K_2O	20.71	21.16	20.93	18.78	22.04	19.52	19.60	20.60	11.47	17.84	19.77	20.63
Total	99.23	99.69	99.06	99.54	99.72	99.91	99.16	100.47	97.44	99.07	100.09	99.82
					Cations per 6 O							
Framework												
Si	2.020	2.015	2.013	2.025	2.008	2.107	2.019	2.014	1.801	2.084	2.017	2.029
Al	0.969	0.967	0.971	0.979	0.952	0.975	0.994	0.983	0.813	0.87	0.970	0.947
Ti	-	-	0.003	-	0.002	0.004	-	0.002	0.033	-	-	-
Fe^{3+}	0.012	0.013	0.017	0.009	0.011	0.014	0.011	0.011	0.340	0.02	0.016	0.028
$\Sigma_{Framework}$	3.001	2.995	2.033	3.013	2.973	3.011	3.024	3.010	2.987	2.975	3.003	3.004
Extra-framework												
Mg	0.003	0.005	-	-	0.004	-	-	-	0.214	0.022	-	-
Mn	-	-	-	-	-	-	-	-	0.010	-	-	-
Ca	-	-	-	-	0.011	-	-	-	0.042	0.020	-	-
Ba	0.001	0.001	0.001	0.002	-	0.003	0.001	0.001	0.005	0.001	0.002	0.001
Na	0.005	0.004	0.004	0.068	0.011	0.042	0.003	0.006	0.110	0.087	0.061	0.004
K	0.946	0.984	0.978	0.863	1.032	0.898	0.905	0.944	0.553	0.820	0.910	0.955
$\Sigma_{Extraframework}$	0.955	0.994	0.983	0.933	1.058	0.943	0.909	0.951	0.934	0.950	0.973	0.960

* Total Fe as Fe_2O_3

Inclusions are generally not suitable for analysis by electron microprobe due to the excitation of the enclosing leucite. In the studied samples, the inclusions are large enough for chemical analyses. They are typically Fe-rich (up to ~12.0 wt% Fe_2O_3) and with significant contents of Mg (~4.0 wt% MgO), Ti (up to ~1.2 wt% TiO_2) Ca (~1.0 wt% CaO) and Na (~1.5 wt% Na_2O), whereas a depletion in Si (~47.6 wt% SiO_2), Al (~18.3 wt% Al_2O_3), and K (~11.5 wt% K_2O) can be observed.

Plagioclase is widely present in the 1872 lithologies and occurs as phenocrysts and in groundmass of lava rocks and clastic fractions. Chemical composition of HL and CL plagioclases respectively cluster at about $An_{76}Ab_{24}$ and $An_{73}Ab_{26}$ - $An_{80}Ab_{6}$, whereas LMC and C plagioclases display compositions of $An_{81}Ab_{17}$ and $An_{55}Ab_{36}$, respectively (Table 4b). Detectable

TABLE 4
Continued...

(b)

Type	HL	HL	HL	HL	CL	CL	LMC	LMC	LMC	LMC	LMC	C
Sample #	D1381 10930	D1423 10972	D1434 10983	9D	D1403 10953	D1464 11013	D1453 11002	D1460 11009	3D	D1453 11002 *ocellus*	D1453 11002 *ocellus*	D1436 10895
SiO_2	49.20	47.64	65.40	49.06	49.73	49.93	47.48	48.25	65.95	60.25	55.77	52.71
Al_2O_3	31.65	32.21	19.10	30.57	31.48	31.57	32.67	32.69	17.97	22.39	26.40	29.03
Fe_2O_3*	0.96	0.76	0.23	0.88	0.67	0.70	0.76	0.70	0.29	0.81	0.76	0.95
CaO	14.40	16.81	0.50	14.74	14.49	14.76	16.74	14.76	1.32	5.51	9.76	11.58
SrO	0.23	-	-	0.38	-	-	0.14	0.43	-	0.08	0.03	0.09
BaO	0.14	-	0.30	0.20	-	-	0.07	0.19	-	1.06	0.08	0.26
Na_2O	2.95	1.90	2.16	2.69	2.85	0.58	1.59	2.18	0.40	3.40	4.72	4.25
K_2O	0.35	0.19	12.43	0.49	0.23	2.19	0.22	0.36	13.86	6.49	1.81	1.46
Total	99.88	99.51	100.12	99.01	99.45	99.73	99.67	99.56	99.79	99.99	99.33	100.33
Cations per 32 O												
Si	9.041	8.809	11.925	9.119	9.130	9.170	8.767	8.896	12.084	11.030	10.180	9.615
Al	6.855	7.020	4.104	6.670	6.811	6.834	7.110	7.103	3.881	4.831	5.680	6.241
Fe^{3+}	0.133	0.106	0.032	0.123	0.093	0.097	0.106	0.097	0.040	0.112	0.104	0.130
Ca	2.835	3.330	0.098	2.935	2.850	2.904	3.312	2.916	0.259	1.087	1.909	2.263
Sr	0.025	-	-	0.041	-	-	0.015	0.046	-	0.009	0.003	0.010
Ba	0.010	-	0.021	0.015	-	-	0.005	0.014	-	0.076	0.006	0.019
Na	1.051	0.681	0.764	0.969	1.014	0.207	0.569	0.779	0.142	1.207	1.670	1.503
K	0.082	0.045	2.891	0.116	0.054	0.523	0.052	0.085	3.240	15.16	0.421	0.340
Σ	20.032	19.991	19.835	19.988	19.952	19.725	19.936	19.936	19.646	19.860	19.974	20.120
Z	16.029	15.935	16.061	15.912	16.030	16.100	15.983	16.097	16.005	15.972	15.964	15.986
X	4.003	4.056	3.774	4.076	3.919	3.250	3.953	3.390	3.641	3.880	4.010	4.134
Ab	26.3	16.8	20.3	23.8	25.9	5.7	14.4	20.3	3.9	31.0	41.7	36.4
An**	71.4	82.1	2.6	73.0	72.7	80.1	84.2	77.1	7.1	28.0	47.7	55.0
Or	2.0	1.1	76.6	2.9	1.4	14.2	1.3	2.2	89.0	39.0	10.5	8.2
Cn	0.3	0.0	0.6	0.4	-	-	0.1	0.4	-	2.0	0.1	0.4

* Total Fe as Fe_2O_3; ** An = $CaAl_2Si_2O_8$ + $SrAl_2Si_2O_8$.

amounts of Ba, Sr and Fe were found in many samples. On the whole, plagioclase compositions plot in the field of those found in 1631-1944 lavas (Fig. 6). Feldspatic *ocelli* (~$An_{38}Ab_{36}$) are observed in HL and mainly in LMC types. Alkali feldspars (sanidine) are restricted to few HL types (~$Ab_{20}Or_{77}$) and in pumice-like LMC rocks (~Ab_4Or_{84}).

Chemical compositions of other silicate minerals in HL, CL, LMC and C types are shown in TABLE 5. Olivine sporadically occurs, partly altered, in HL lava samples and fragments of C type; in the first ones, it can present a core to rim trend of Fo_{97} to Fo_{89} (TABLE 5a). Small amounts of Ti, Cr, Al, Mn, Mg and Ca are detected. Osumilite and indialite compositions, with their high Mg

contents and significant amounts of K (Table 5a), are comparable to those recently detected in other 1872 samples (Balassone *et al.,* 2004; 2008. See these papers for a more detailed description of this mineral assemblage). In HL and LMC lithologies, sodalite-group minerals are quite diffuse and correspond to sodalite and noseane. The range of most significant cations, expressed in apfu, are in the ranges Na 7.68-6.43, Ca 0.01-0.85, K 0.01-0.40; anions vary in the ranges Cl 1.59-2.16, SO_4 0.01-0.85 and F 0.03-0.10 apfu (Table 5b and Fig. 7a). LMC cancrinite-group minerals display have been characterized as quadridavyne, microsommite and afghanite; plotted in the Ca+K *vs* Na+S diagram, compositional features are quite similar to Somma-Vesuvius cancrinites from bibliography (Fig. 7b and Table 5b). SEM micrographs of typical cancrinite minerals are shown in Fig. 8. X-ray analyses have also demonstrated the presence of trace amounts of davyne in sample E5877 17337 (Ballirano, personal communication).

Chemical compositions of non silicate minerals are presented in Table 6. Iron oxides, magnetite and hematite, are quite ubiquitous in these lithologies, both in lava groundmass and as euhedral crystals in interstices, fractures and cavity linings (Table 6a). HL magnetite is Ti-rich (up to ca. 22.0 wt% TiO_2) compared to those from other types (maximum value detected ca. 7.0 wt% TiO_2). Significant contents of Al (max. 3.8 wt% Al_2O_3), Mg (max. 3.8 wt% MgO) and Mn (max.1.3 wt% MnO) are found in all phases, whereas Cr and Ca are present in traces. Hematite

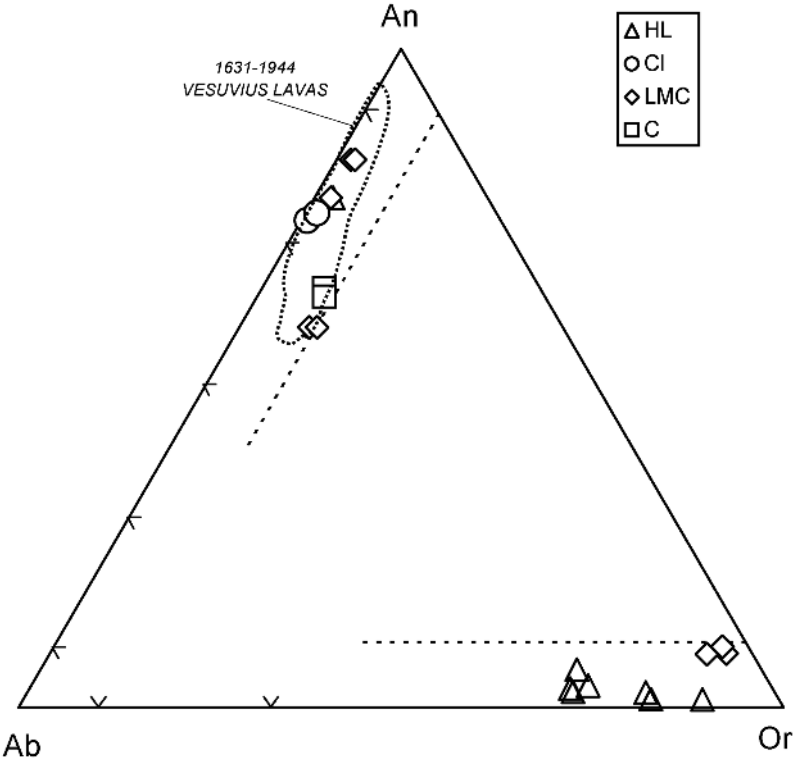

Fig. 6 - Ab-An-Or diagram for feldspars from Somma-Vesuvius 1872 samples. The dotted field shows the composition of plagioclase from 1631-1944 vesuvian lavas after Solone (2006).

from LMC can be enriched in Al and Ti (up to ~ 3.8 wt% Al_2O_3 and ~ 2.0 TiO_2 wt%, respectively) compared to the other phases, with trace amounts of Mg, Mn and Cr. Apatite was locally detected in HL, CL and LMC types; it is generally a fluoroapatite, locally with values up to 1.6 wt% V_2O_5 and small amounts of REE (TABLE 6b). Ca-sulfates (gypsum and anhydrite) and halite (sylvite is sporadically found as well) can mainly occur as tiny crystal on the sample vugs and/or surfaces (TABLE 6b).

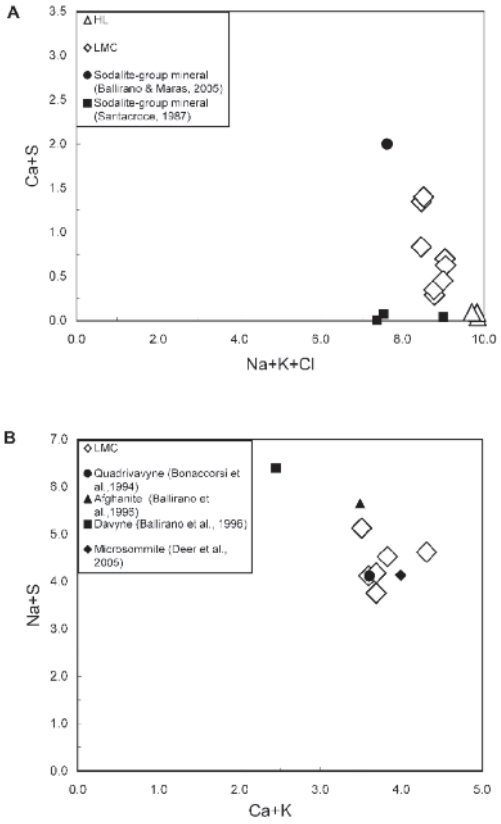

Fig. 7 - **A** Plot of Na+K+Cl *vs* Ca+S in apfu for sodalite-group minerals from the investigated rocks, compared to those from selected bibliography. **B** Ca+K *vs* Na+S (apfu) diagram for cancrinite-group minerals of 1872 samples; some reference data for Somma-Vesuvius cancrinites are also reported.

DISCUSSION AND CONCLUSIONS

The ejected rocks of Somma-Vesuvius 1872 eruption studied for the present research show variations in relation to textures/microtexures and mineralogical features.

Textural and petrographic observations strongly suggest that lava sequences of Vesuvius, mainly leucititic tephrites and tephritic phonolites, form the whole of HL and CL rocks and most of lithics and loose crystal components (mainly clinopyroxene and leucite) found in LMC and C ejecta. Typical conglomeratic and often friable textures of LMC and C types, as well as and their crystal fractions, are likely due to disaggregation and hydrothermal alteration which affected to various extent early-formed lava protholits. Petrographic evidences show that fine-grained matrix found in LMC and C type is mainly composed by a mineral association genetically related to late to post-magmatic crystallization.

Mineral chemistry investigation has shown that the 1872 ejected rocks consist of a large number of phases. These include minerals which typically occur in the Somma-Vesuvius lavas, like clinopyroxene, leucite (and other feldspathoids) and plagioclase and most of potassic feldspar, phlogopite as well.

A detailed examination of variations in mineral compositions and occurrence mode can provide further information on minerogenetic processes concerning the 1872 ejected rocks. Ubiquitous clinopyroxene is compositionally similar to those from historical lavas; corrosion and reaction rim evidences can indicate resorption processes due to changing physico-chemical conditions (e.g. variable silica activity). According to Morgan *et al.* (2004), chemical zoning observed in these mineral phases represented by hedenbergite-rich core and salite-rich rim (as observed in some LMC sample) can be related to a superficial magma chamber, whereas individuals with

Table 5

Chemical analyses of miscellaneous silicates detected in HL and LMC lithotypes: (a) olivine, Ol, osumilite, Osm, indialite, Ind, and cristobalite, Crs; (b) sodalite-group minerals, Sdl, and cancrinite-group minerals, Ccn.

(a)

Type	HL	HL	HL		LMC	LMC		LMC	LMC	LMC
Mineral	Ol	Ol	Ol		Os	Os		Ind	Ind	Crs
Sample #	D1381 10930 core	D1381 10930 rim	D1434 10983		3D	3D		3D	3D	3D
SiO_2	41.89	39.89	40.70	SiO_2	62.00	61.91		48.24	48.33	94.86
TiO_2	0.06	-	0.03	TiO_2	0.08	0.14		-	0.11	0.11
Al_2O_3	0.12	0.03	-	Al_2O_3	23.16	22.96		35.12	35.21	1.25
Cr_2O_3	-	0.04	-	FeO*	1.78	1.83		0.66	0.75	0.32
FeO*	2.19	9.19	11.3	MgO	8.11	7.95		13.59	12.96	0.06
MnO	0.87	1.07	0.19	CaO	0.17	0.18		0.73	0.19	0.09
MgO	53.19	48.16	47.7	Na_2O	0.14	0.31		0.20	0.40	0.19
CaO	0.83	2.43	0.31	K_2O	4.01	4.68		1.01	1.36	0.40
Total	99.15	100.81	100.23	Total	99.45	99.96		99.55	99.31	97.28
		4 O		**17 framework cations (Si, Al, Fe, Mn, Mg, Ti)**					**18 O**	
Si	1.004	0.980	1.002	Si	10.240	10.272	Si	4.797	4.820	-
Al	0.003	0.001	0.001	Al	1.760	1.728	Al	4.117	4.139	-
Ti	0.001	-	0.001	S	12.000	12.000	Ti	-	0.008	-
Cr	-	0.001	-	Al	2.747	2.762	Fe”	0.055	0.063	-
Fe_t	0.044	0.189	0.233	Fe”	0.246	0.254	Mg	2.015	1.927	-
Mn	0.018	0.022	0.004	Mg	1.997	1.967	Ca	0.077	0.020	-
Mg	1.901	1.763	1.750	Ti	0.010	0.017	Na	0.039	0.077	-
Ca	0.021	0.064	0.008	S	5.000	5.000	K	0.128	0.173	-
$\Sigma_{cations}$	1.988	2.040	1.997	Ca	0.030	0.032	$\Sigma_{cations}$	11.228	11.227	-
				Na	0.045	0.100				
				K	0.845	0.991				
				S	0.920	1.123				
*mg***	0.969	0.893	0.881		0.890	0.886		0.973	0.969	

* Total iron as FeO; *mg***=Mg/(Mg+Fe_t+Mn).

diopsidic core can form at higher depth.

Mica has a phlogopitic composition, most of them with quite similar values in term of Mg/Fe ratio and TiO_2 contents. Only one HL rock and particularly pumice-like LMC mica grains display higher Mg/Fe ratios and lower TiO_2. According to Fulignati *et al*. (1998), low-Ti phlogopites are typical of Somma-Vesuvius skarns or of high temperature hydrothermal systems. The presence in many samples of micas in groundmass, in some case also corroded, indicates high volatile contents in the melts (e.g. H_2O, F; Aurisicchio *et al.,*1988). The prominent role of water in the magmatic evolution is supported by significant fluorine amount observed in many 1872 rock-forming minerals and by the explosive feature of the Vesuvius volcanic activity.

Widespread leucite are often characterized by coronae and/or radial, Fe-rich, dark inclusions. They could be ascribed to a series of processes,

TABLE 5
Continued...

(b)

Type	HL	LMC	LMC	LMC	LMC	LMC	LMC	LMC	LMC	LMC	LMC
Mineral	Sdl	Sdl	Sdl	Sdl	Sdl	Ccn	Ccn	Ccn	Ccn	Ccn	Ccn
Sample #	D1400	D1502	D1502	E5652	3D	D1520	E5876	E5876	E5877	E5877	3D
	10949	11051	11051	17113		11051	17337	17337	17338	17338	
SiO_2	38.69	36.65	35.51	36.58	38.28	33.09	33.87	33.16	31.41	33.07	30.44
Al_2O_3	29.98	30.56	29.54	29.97	30.64	27.62	27.07	25.63	24.95	25.79	27.34
TiO_2	0.01	0.04	-	0.07	-	-	-	-	-	-	-
Fe_2O_3*	0.39	0.60	0.74	0.95	0.36	-	-	0.78	0.66	0.76	0.10
MgO	-	0.04	-	0.03	0.02	-	-	0.03	0.19	0.08	0.04
CaO	0.08	2.69	4.70	3.08	1.62	11.35	9.48	10.90	13.54	11.58	12.27
Na_2O	24.45	21.51	19.74	20.07	21.21	11.21	10.49	11.63	7.96	9.86	10.71
K_2O	0.10	1.09	1.83	1.70	0.37	5.93	7.92	5.54	5.95	6.32	4.86
SO_3	0.20	1.24	3.90	2.34	0.07	1.08	0.31	6.38	10.90	6.73	1.43
Cl	7.88	7.15	5.53	5.99	7.70	12.13	12.09	7.75	4.55	6.80	12.75
F	0.09	0.14	0.06	0.06	0.20	-	-	-	0.19	0.09	-
Total	101.87	101.71	101.55	100.84	100.47	102.41	101.23	101.80	100.30	101.08	99.94
-O=Cl.F	1.81	1.67	1.27	1.37	1.82	2.73	2.72	1.75	1.11	1.57	2.87
Tot	100.06	100.04	100.28	99.47	98.65	99.68	98.51	100.05	99.19	99.51	97.07
					12 T-cations						
Si	6.246	6.012	6.011	6.040	6.152	6.049	6.179	6.222	6.147	6.197	5.822
Al	5.705	5.909	5.894	5.833	5.804	5.951	5.821	5.668	5.756	5.696	6.164
Ti	0.001	0.005	-	0.009	-	-	-	-	-	-	-
Fe^{3+}	0.048	0.074	0.064	0.118	0.044	-	-	0.110	0.097	0.107	0.014
Mg	-	0.010	-	0.007	0.005	-	-	0.008	0.055	0.022	0.011
Ca	0.014	0.471	0.849	0.543	0.278	2.213	1.845	2.182	2.827	2.315	2.503
Na	7.684	6.842	6.480	6.426	6.610	3.973	3.711	4.231	3.021	3.583	3.972
K	0.005	0.228	0.395	0.358	0.076	1.383	1.843	1.326	1.486	1.511	1.186
SO_4	0.024	0.153	0.496	0.290	0.008	0.148	0.042	0.898	1.601	0.947	0.205
Cl	2.156	1.988	1.587	1.676	2.097	3.758	3.738	2.465	1.509	2.160	4.133
F	0.046	0.073	0.032	0.031	0.102	-	-	-	0.118	0.053	-
$\Sigma_{cations}$	7.688	7.551	7.724	7.334	6.968	7.570	7.399	7.747	7.389	7.430	7.673
Σ_{anions}	2.226	2.213	2.114	1.998	2.208	3.906	3.781	3.363	3.228	3.160	4.339

* Total iron as Fe_2O_3.

like variable crystal growth and/or stability due to changes in pressure conditions related to explosive events, to magma mixing or to the occurrences of convective cells into magma chambers.

K-feldspar *ocelli* as well can be related to differentiation processes occurring in basic alkaline-potassic magma to form more felsic compositions, through fractionation of cumulate crystals, like clinopyroxene, leucite and plagioclase.

Amphiboles can mantle clinopyroxene cores and mainly occurs as fracture and cavity filling and in the matrix of LMC rocks, suggesting a late- to post-magmatic crystallization.

Another particular feature of the investigated

Table 6

Chemical composition of miscellaneous non silicates locally found in the 1872 lithotypes: (a) magnetite, Mgt, and hematite, Hem; (b) apatite, Ap, anhydrite, Anh, gypsum, Gp, and halite, Hl.

(a)

Type	HL	HL	CL	CL	LMC	LMC	LMC	LMC		HL	HL	LMC	LMC	C
Mineral	Mgt	Mgt	Mgt	Mgt	Mgt	Mgt	Mgt	Mgt		Hem	Hem	Hem	Hem	Hem
Sample #	D1400	D1468	D1418	D1418	D1422	D1453	D1453	5652		D1468	D1468	D1460	D1460	D1436
	10949	11017	10967	10967	10971	11002	11002	17113		11017	11017	11009	11009	10895
SiO_2	0.35	0.69	0.07	0.05	0.10	0.04	0.03	0.09	TiO_2	0.06	-	2.07	0.19	0.43
TiO_2	21.51	10.21	6.74	6.88	6.09	4.75	5.20	6.62	Al_2O_3	0.65	0.54	3.73	1.17	1.02
Al_2O_3	2.09	3.83	1.07	1.15	0.69	1.23	1.18	0.99	Cr_2O_3	0.05	0.01	0.08	0.05	0.08
Cr_2O_3	-	0.02	0.07	0.14	-	0.02	0.07	0.07	Fe_2O_3***	98.67	98.92	91.91	97.15	97.97
FeO*	72.00	77.55	80.97	80.54	82.87	85.06	84.56	82.20	MnO	0.30	-	0.86	0.16	0.11
MnO	0.78	1.00	1.00	1.12	1.33	0.36	0.37	1.13	MgO	0.01	0.12	1.00	0.50	0.24
MgO	0.37	1.05	2.76	2.89	3.01	2.04	2.08	2.87	*Total*	*99.74*	*99.59*	*99.65*	*99.22*	*99.85*
CaO	0.16	0.22	0.03	0.11	0.05	0.11	0.07	0.06						
Total	97.26	94.57	92.71	92.88	94.14	93.61	93.56	94.03						
Fe_2O_3**	24.19	42.97	54.72	54.33	57.76	59.04	58.12	56.07						
FeO**	50.23	38.89	31.73	31.48	30.89	31.94	32.27	31.74						
Total	*99.68*	*98.88*	*98.19*	*98.34*	*99.93*	*99.53*	*99.38*	*99.65*						
				32 O										
Si	0.104	0.206	0.021	0.015	0.030	0.012	0.009	0.027						
Al	0.734	1.347	0.382	0.410	0.243	0.437	0.419	0.349						
Cr	-	0.005	0.017	0.033	-	0.005	0.017	0.017						
Fe^{3+}	5.421	9.6510	12.484	12.399	12.965	13.382	13.187	12.606						
Ti	4.818	2.292	1.537	1.564	1.366	1.076	1.179	1.488						
Fe^{2+}	12.511	9.708	8.044	7.955	7.706	8.045	8.136	7.931						
Mn	0.197	0.253	0.257	0.287	0.336	0.092	0.094	0.286						
Mg	0.164	0.467	1.247	1.302	1.338	0.916	0.935	1.278						
Ca	0.051	0.070	0.010	0.036	0.016	0.036	0.023	0.019						

* Total Fe as FeO; ** recalculated according to Stormer (1983); *** Total Fe as Fe_2O_3.

TABLE 6
Continued...

(b)

Type	HL	CL	CL	LMC	LMC		HL	HL	HL	CL		HL	HL
Mineral	Ap	Ap	Ap	Ap	Ap		Anh	Anh	Gp	Gp		Hl	Hl
Sample #	7D	D1403 10953	D1418 10967	5652 17113	3D		D1468 11017	9D	D1467 11016	D1464 11013		D1423 10972	9D
P_2O_5	42.51	41.15	39.49	39.11	41.46	SiO_2	-	0.15	-	0.13	Na	38.91	37.99
V_2O_5	-	-	1.05	1.64	0.10	Al_2O_3	0.03	0.03	-	0.07	K	0.43	0.66
SiO_2	0.49	0.44	0.65	0.75	0.40	Fe_2O_3**	0.07	-	0.05	0.11	Ca	0.17	0.67
FeO*	0.28	0.21	0.28	0.27	0.38	MgO	0.05	0.02	0.99	0.45	Mg	0.12	0.14
CaO	53.15	54.92	53.74	55.15	52.10	CaO	41.68	40.45	33.06	32.39	Cl	60.11	60.23
MnO	-	0.24	0.09	0.10	-	SrO	0.12	0.33	0.12	0.32	SO_4	0.23	0.16
SrO	0.31	0.28	0.07	0.15	0.05	BaO	0.08	0.18	0.05	0.13		99.97	99.85
Na_2O	0.03	0.04	0.05	0.05	0.23	Na_2O	0.05	0.06	0.03	-			
K_2O	0.02	-	0.15	-	0.23	K_2O	0.05	-	0.05	0.09			
F	3.06	3.19	4.26	3.48	3.41	SO_3	56.58	56.99	46.22	45.37			
Cl	0.63	0.52	0.19	0.20	1.11	*Total*	*98.71*	*98.21*	*80.57*	*79.06*			
Total	*100.48*	*100.99*	*100.02*	*100.90*	*99.47*								
-O=F.Cl	1.43	1.46	1.84	1.51	1.69								
Total	*99.05*	*99.53*	*98.18*	*99.39*	*97.78*								
			26 (O, F, Cl)				**4 O in the anhydrous molecule**						
P	6.087	5.925	5.752	5.684	6.022	Si	-	0.003	-	0.004			
V	-	-	0.145	0.226	0.012	Al	0.001	0.001	-	0.002			
Si	0.083	0.075	0.112	0.129	0.069	Fe’’’	0.001	-	0.001	0.002			
Fe_t	0.040	0.030	0.040	0.039	0.055	Mg	0.002	0.001	0.042	0.019			
Ca	9.631	1.001	9.907	10.144	9.578	Ca	1.036	1.006	1.004	1.004			
Mn	-	0.035	0.013	0.015	0.001	Sr	0.002	0.004	0.002	0.005			
Na	0.010	0.013	0.017	0.017	0.077	Ba	0.001	0.002	0.001	0.001			
K	0.004	-	0.033	-	0.050	Na	0.002	0.003	0.002	-			
F	1.637	1.716	2.318	1.889	1.850	K	0.001	-	0.002	0.003			
Cl	0.181	0.150	0.055	0.058	0.323	S	0.985	0.993	0.983	0.985			

* Total Fe as FeO; ** Total Fe as Fe_2O_3.

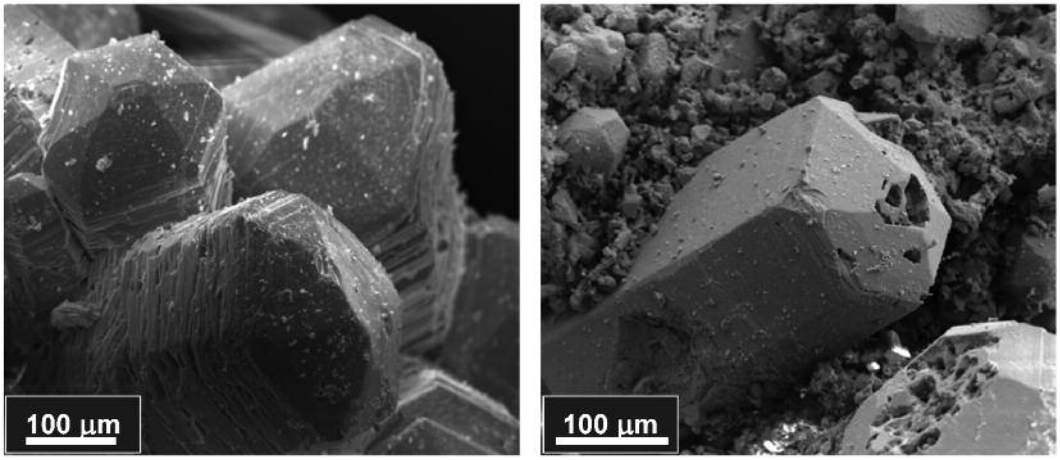

Fig. 8 - SEM micrographs of cancrinite-group minerals of LMC samples.

ejecta is the occurrence of many mineral phases containing volatile species among their main components. The composition of these phases indicates the presence of a fluid phase with high amounts of fluorine, sulphur and chlorine. The high fluorine activity is testified by significant contents of micas, amphibole and apatite. Sodalite- and cancrinite-group minerals show trace amounts of F as well. The high sulphur fugacity is demonstrated by the widespread occurrence of cancrinite-group minerals and Ca-sulfates (gypsum and anhydrite). SO_3 is also detected in remarkable amounts in sodalite-group minerals and in traces in apatite. Crystallization of sodalite minerals, halite and sylvite are related to high Cl activity fluids. Moreover, the occurrence of detectable amounts of Ba, Sr and REE in many mineral phases (together with other trace elements, like vanadium in apatites) testifies to a concentration of these elements in the system, likely due to enrichment in incompatible elements of the potassic magma reservoir.

Iron oxides mainly crystallize in sample vugs, interstices and surfaces and can generally testify high oxygen fugacity and a late- to post-magmatic genesis.

In conclusion, textural, petrographic and mineral chemistry evidences indicate that phase crystallization has occurred by a number of processes and complex interactions between rising lava, lava protholits and pulse of hydrothermal fluids and fumaroles at variable temperature and composition. Minerogenetic processes include crystallization from magma, metasomatism by fluids, reaction between various minerals and new fluid-rich melts and late to post deposition from circulating fluid phases. In particular, lava, scoriae and pumice lithics represent Vesuvius protholits which were affected by fragmentation to various degrees, to form the different lithologies HL, CL, LMC and C. Low temperature chlorine- and sulphur-rich brines concentrated by volcanic heating as well as fumarolic emissions can be responsible for crystallization of sulphates, halides and partly of Fe-oxides.

Acknowledgements

This study was carried out in the frame of L.R.-BURC 2005-2007 Research Projects funded to M.R. Ghiara. M. Serracino (IGAG CNR, Rome) and R. dé Gennaro (CISAG, University “Federico II”, Naples) are heartily thanked for their skilful technical assistance

during WDS and SEM-EDS analyses, respectively. We are also indebted to A. De Stefano, M. Lindinerro and P. Tortora for helping with analytical work. P. Brotzu and L. Cirrincione are thanked for constructive comments. We wish to thank A. Gianfagna for useful suggestions and the editorial assistance. P. Ballirano (University "La Sapienza", Rome) is acknowledged for performing X-ray analyses of two cancrinite samples.

REFERENCES

Ayuso R.A., De Vivo B., Rolandi G., Seal R. II and Paone A. (1998) - *Geochemical and isotopic (Nd-Pb-Sr-O) variations bearing on the genesis of volcanic rocks from Vesuvius, Italy*. J Volcanol. Geotherm Res., **82**, 53-78

Arno' V., Principe C., Rosi M., Santacroce R., Sbrana, A. and Sheridan M. F. (1987) - *Somma-Vesuvius eruptive history.* Quaderni de 'La Ricerca Scientifica' XIII, 53-103.

Aurisicchio C., Federico M. and Gianfagna A. (1988) - *Clinopyroxene chemistry of the high-potassium suite from the Alban Hills, Italy*. Mineral. Petrol., **39**, 1-19.

Balassone, G., Franco, E., Mattia, C. A. and Puliti, R. (2004) - *Indialite in xenolithic rocks from Somma-Vesuvius volcano (southern Italy): crystal chemistry and petrogenetic features*. Am. Mineral., **89**, 1-6.

Balassone G., Mormone A., Rossi M. Bernardi A., Fisch M., Armbruster T., Malsy A. K. and Berger A. (2008) - *Crystal chemical and structural characterization of an Mg-rich osumilite from Vesuvius volcano (Italy).* Eur.J. Mineral., **20**, 713-720.

Ballirano P., Maras A. and Buseck P.R. (1996) - *Cystal chemistry and IR spectroscopy of Cl- and SO_4- bearing cancrinite-like minerals.* Am. Mineral., **81**, 1003-1012.

Ballirano P. and Maras A. (2005) - *Crystal chemical and structural characterization of an unusual CO_3-bearing sodalite-group mineral.* Eur. J. Mineral., **17**, 805-812.

Bonaccorsi E., Merlino S., Orlandi P., Pasero M. and Vezzalini G. (1994) - *Quadridavyne, [(Na, K)$_6$Cl$_2$[Ca$_2$Cl$_2$][Si$_6$Al$_6$O$_{24}$], a new feldspathoid mineral from Vesius area.* Eur. J. Mineral., **6**, 481-487.

Cigolini C. (2007) - *Petrography and thermobarometry of high-pressure ultramafic ejecta from Mount Vesuvius, Italy: inferences on the deep feeding system*. Per. Mineral., **76**, 5-24.

Cioni R., Marianelli P. and Santacroce R. (1998) - *Thermal and compositional evolution of the shallow magma chambers of Vesuvius: evidence from pyroxene phenocrysts and melt inclusions*. J. Geophys. Res., **103**, 18277-18294.

Conticelli S., D'Antonio M., Pinarelli L. and Civetta L. (2002) - *Source contamination and mantle heterogeneity in the genesis of Italian potassic and ultrapotassic volcanic rocks: Sr-Nd-Pb data frm Roman Province and Southern Tuscany*. Mineral. Petrol., **74**, 189-222.

Di Renzo V., Di Vito M. A., Arienzo I., Carandente A., Civetta L., D'Antonio M., Giordano F., Orsi G. and Tonarini F. (2005) - *Magmatic history of Somma-Vesuvius on the basis of new geochemical and isotopic data from a deep borehole (Camaldoli della Torre)*. J. Petrol., **48**, 753-784.

Droop G.T.R. (1987) - *A general equation for estimating Fe^{3+} concentrations in ferromagnesian silicates and oxides from microprobe analyses, using stoichiometric criteria.* Mineral. Mag., **51**, 431-453.

Federico M. and Peccerillo A. (2002) - *Mineral chemistry and petrogenesis of granular ejecta from the Alban Hills volcano (Central Italy).* Mineral. Petrol., **74**, 223-252.

Fulignati P., Marianelli P. and Sbrana A. (1998) - *New insight on the thermo-metasomatic magma chamber shell of the 1944 eruption of Vesuvius.* Acta Vulc., **10**, 47-54.

GE Inspection Technologies (2004) - *RayfleX - Version 2.336.* GE Inspection Technologies, USA-Germany.

Ghiara M.R. (2005) - *Indagini minero-petrografiche e geochimiche sulle associazioni paragenetiche presenti nei proietti dell'eruzione del 1872 del Somma-Vesuvio: definizioni delle condizioni chimico-fisiche che hanno sovrinteso alla minerogenesi*. Scientific Report L.R. *5/2002*, 1-85.

Gilg A.H., Lima A., Somma R., Belkin H.E., De Vivo B. and Ayuso R.A. (2001) - *Isotope geochemistry and fluid inclusion study of skarns form Vesuvius*. Mineral. Petrol., **73**, 145-176.

Guidotti C. V. (1984) - *Micas in metamorphic rocks.* In: Bailey, S. W. (ed.) Micas. Mineralogical Society of America. Rev. Mineral. Geochem., **13**, 357-467.

Joron J. L., Metrich N., Rosi M., Santacroce R. and Sbrana A. (1987) - *Chemistry and petrography.* In: Santacroce, R. (ed.) Somma-Vesuvius. Quaderni de 'La Ricerca Scientifica' **114**, 105-174.

Kretz R. (1983) - *Symbols for rock-forming minerals*. Am. Mineral., **68**, 277-279

Leake B.E., Woolley A.R., Arps C.E.S, Birch W.D., Gilbert M.C., Grice J.D, Hawthorne F.C., Kato A., Kisch H.J., Krivovichev V.G., Linthout K., Laird J., Mandarino J.A., Maresch W.V., Nickel E.H., Rock N.M.S., Schumacher J.C., Smith D.C., Stephenson N.C.N., Ungaretti L., Whittaker E.J.W. and Guo Y. (1997) - *Nomenclature of amphiboles of the International Mineralogical Association. CNMMN, IMA*. Am. Mineral., **82**, 1019-1037.

Leake B.E., Woolley A.R., Birch W.D., Burke E.A.J., Ferraris G., Grice J.D., Hawthorne F.C., Kisch H.J., Krivovichev V.G., Schumacher J.C., Stephenson N.C.N. and Whittaker E.J.W. (2004) - *Nomenclature of amphiboles: additions and revisions to the International Mineralogical Association's amphibole nomenclature.* Am. Mineral., **88**, 883-887.

Lima A., De Vivo B., Fedele L., Sintoni F. and Milia A. (2007) - *Geochemical variations between the 79 A.D. and 1944 A.D. Somma-Vesuvius volcanic products: constraints on the evolution of hydrothermal system based on fluid and melt inclusions.* Chem. Geol., **237**, 401-417.

Lirer L., Chirosca M.C., Munno R., Petrosino P. and Grimaldi M. (2005) - *Il Vesuvio. Ieri, Oggi, Domani.* Regione Campania, Napoli, 150 pp.

Marianelli P., Metrich N. and Sbrana A. (1999) - *Shallow and deep reservoirs involved in the magma supply of the 1944 eruption of Vesuvius*. Bull.Volcanol., **61**, 48-63.

Mitchell R.H. (1991) - *Coexisting glasses occurring as inclusions in the leucite from lamproites: examples of silicate liquid immiscibility in ultrapotassic magmas*. Mineral. Mag., **55**, 197-202.

Morimoto N., Fabries J., Ferguson A.K., Ginzburg I.V., Ross M., Seifert F.A., Zussman J., Aoki K. and Gottardi G. (1988) - *Nomenclature of Pyroxenes. Subc. Pyroxene. CNMMN, IMA*. Mineral. Petrol., **39**, 55-76.

Morgan D.J., Blake S., Rogers N.W., De Vivo B., Rolandi G., MacDonald R. and Hawkesworth C.J. (2004) - *Time scale of crystal residence and magma chamber volume from modelling of diffusion profiles in phenocrysts: Vesuvius 1944*. Earth Planet. Sci. Lett., **222**, 933-946.

Oxford Instrument (2006) - *INCA - The microanalysis suite issue 17a+SP1 - Version 4.08*. Oxford Instr. Anal. Ltd., Oxfordshire, UK.

Palmieri L. (1872) - *Dell'incendio vesuviano del 26 aprile 1872*. Atti R. Acc. Sci. B. Lett. Napoli, An. IX, 157-158.

Palmieri L. (1873) - *Incendio Vesuviano del dì 26 Aprile del 1872*. Atti R. Acc. Sci. Fis. Nat. Napoli, 5-17.

Palmieri L. (1874) - *L'incendio vesuviano del 26 aprile 1872*. Ann. R. Oss. Ves., Anno I , 5-103.

Papike J.J., Cameron K.L. and Baldwin K. (1974) - *Amphiboles and pyroxenes; characterization of other than quadrilateral components and estimates of ferric iron from microprobe data*. Geol. Soc. Amer. Abs. Prog., **6**, 1053-1054.

Parodi G.C., Ballirano P. and Maras A. (1996) - *Afghanite from Mount Vesuvius: a rediscovery.* Min. Rec., **27**, 109-114.

Petti C., Balassone G., Bernardi A., Mormone A. and Rossi M. (2008) - *I reperti dell'eruzione vesuviana del 1872 della "Collezione Scacchi" (Real Museo Mineralogico di Napoli)*. In "Somma-Vesuvio e Real Museo Mineralogico", M.R Ghiara., ed.,. Medias, Napoli, 42-61.

Pouchou J.L. and Pichoir F. (1991) - *Quantitative analysis of homogeneous or stratified microvolumes applying the model "PAP".* Electron Probe Quantitation, Eds. Heinrich & Newbury, Plenum Press N.Y., 31-75,

Rieder M., Cavazzini G., D'yakonov Y.S., Frank Kamenetskii V.A., Gottardi G., Guggenheim S., Koval P.V., Muller G., Neiva A.M.R., Radoslovich E.W., Robert J.L., Sassi F.P., Takeda H., Weiss Z. and Wones D.R. (1998) - *Nomenclature of the micas*. Clays Clay Miner., **46**, 586-595.

Rolandi G., Barrella A. M. and Borrelli A. (1993) - *The 1631 Eruption of Vesuvius.* J. Volcanol. Geotherm. Res., **58**, 183-201.

Russo M. and Punzo I. (2004) - *I minerali del Somma-Vesuvio.* AMI, Cremona, 320 pp.

Santacroce R., (1987). *Somma-Vesuvius.* Quaderni de 'La Ricerca Scientifica', **114**(8), 230 pp.

Santacroce R., Cioni R., Marianelli P. and Sbrana

A. (2005) - *Understanding Vesuvius and preparing for its next eruption*. In: Balmuth, M. S., Chester D. K. & Johnston, P. A. (eds) Cultural Responses to the Volcanic Landscape. The Mediterranean and Beyond. Archaeological Institute of America, colloquia and Conference Papers, **8**, 27-55.

Scacchi A. (1872a) - *Notizie preliminari di alcune specie mineralogiche rinvenute nel Vesuvio dopo l'incendio di Aprile 1872*. Atti R. Acc. Sci. Fis. Mat. Napoli, **11**, 210-213.

Scacchi A. (1872b) - *Contribuzioni mineralogiche per servire alla Storia dell'incendio vesuviano del mese di aprile 1872*. Parte prima. Atti R. Acc. Sci. Fis. Mat. Napoli, s. 1, vol. 5-22, 1-35.

Scacchi A. (1873) - *Contribuzioni mineralogiche per servire alla Storia dell'incendio vesuviano del mese di aprile 1872*. Parte prima. Atti R. Acc. Sci. Fis. Mat. Napoli, s. 1, vol. 6-9, 1-69.

Scacchi A. (1886) - *Sopra un frammento di antica roccia vulcanica inviluppato nella lava vesuviana del 1872*. Atti R. Acc. Sci. Fis. Mat. Napoli, s. 2, vol. 1-5, 1-19

Scacchi A. (1888) - *Catalogo dei minerali vesuviani.* Atti R. Ist. Inc. Napoli, 1, 1-57.

Scacchi A. and Scacchi E. (1883) - *Sopra un frammento di antica roccia vulcanica inviluppato nella lava vesuviana del 1872*. Atti R. Acc. Sci. Fis. Mat. Napoli, s. 1, vol. 22, 281-283.

Scandone R., Giacomelli L. and Fattori Speranza F. (2006) - *The volcanological history of the volcanoes of Naples: a review*. In B. De Vivo Editor, "Volcanism in the Campania Plain", Developments in Volcanology-9, Elsevier, 1-26.

Solone R. (2006) - *Petrogenesi delle lave potassiche ed ultrapotassiche del Monte Somma (Italia)*. Unpublished PhD Dissertation, University "Federico II", Naples, 134 pp.

Stormer J.C. Jr. (1983) - *The effects of recalculation on estimates of temperature and oxygen fugacity from analyses of multicomponent iron-titanium oxides*. Am. Mineral., **68**, 586-594.